A parametric study on countermeasures to mitigate subway traffic induced vibration and noise in buildings

[1]**P. Fiala,** [2]**S. Gupta,** [2]**G. Degrande,** [1]**F. Augusztinovicz**
[1]Budapest University of Technology and Economics, Department of Telecommunications
Magyar tudósok körútja 2., H-1117, Budapest, Hungary
[2]K.U.Leuven, Department of Civil Engineering,
Kasteelpark Arenberg 40, B-3001, Heverlee, Belgium
e-mail: **fiala@hit.bme.hu**

Abstract
A numerical model is presented to predict the effect of countetrmeasures mitigating subway traffic induced ground-borne noise and vibration in buildings. An invariant concrete tunnel embedded in a layered half space is modelled using the coupled periodic finite element-boundary element approach. The response in the free field due to a moving vehicle is predicted in the frequency range 1-150 Hz, and vibrations in a simple portal frame building are estimated by solving a dynamic soil-structure interaction problem. An acoustic 3D spectral finite element method is used to predict the acoustic response inside the rooms of the building. The methodology is used to investigate the efficiency of a floating slab track in the tunnel, base-isolation of the building and a box-within-box arrangement in the room. It is shown that the insertion gains computed with the complex model significantly differ from those obtaind from simple rules of thumb, and that source isolation is the most effective countermeasure to mitigate ground-borne noise and vibrations.

1 Introduction

Significant vibrations in buildings near railway tracks and subway tunnels are attributed to moving trains. The train moving on an uneven track excites vibrations that are transmitted through the surrounding soil to nearby buildings. These soil vibrations induce structural vibrations that are dominant in the frequency range between 10 Hz and 80 Hz, and the structural vibrations cause re-radiated noise in the building's enclosures. This noise is dominant in the frequency range between 50 Hz and 200 Hz. In dense urban environment, the architectural design process must involve the planning of vibration isolation systems that can mitigate the structural vibrations and re-radiated noise. In order to be able to design vibration isolation countermeasures, prediction tools are needed that can model the vibration propagation from the railway to the structure.

In the present paper, a numerical model is introduced that is capable to handle the complex vibration-propagation problem. The method is introduced in a numerical example, where a hypothetical portal frame building resting on a layered soil is exposed to ground-borne vibrations from underground railway traffic. The insertion gain of three vibration and noise mitigation methods with respect to noise levels is computed.

The problem of vibration propagation from the moving vehicle to the listener in the structure's room can practically be divided into three subproblems. The first subproblem deals with the vibration generation into the soil by moving vehicles on a surface or underground railway track. The second subproblem is the dynamic soil-structure interaction (SSI) problem, where the incident wave field is applied as an excitation to a couped soil-structure model. In this part, the structural vibrations excited by the incident wave field are determined. In the third subproblem, the radiation problem is solved, and the sound pressure radiated into the closed rooms of the structure by vibrating walls is determined.

The methodology is used to classify different measures to mitigate structural vibrations and re-radiated noise. Vibration and noise isolation at three elements of the vibration chain is considered. Firstly, a floating slab track is investigated by modifying the track model in the first subproblem. This countermeasure has the advantage that it reduces the ground vibrations, and yields a global vibration isolation in all the surrounding buildings. The second investigated countermeasure is base isolation of the structure. This is modeled by modifying the structure model in the second subproblem. The last investigated method is a local noise and vibration isolation of a single room in the building, by means of a box-within-box arrangement.

2 The numerical model

The total vibration path is divided into three weakly coupled problems. The first problem is the computation of the free field ground vibrations generated by a metro train running on a periodic track. Within the frame of the CONVURT project, a coupled periodic FE-BE model has been developed to handle this first subproblem. The model accounts for quasi-static and unevenness excitations and takes dynamic track-tunnel and tunnel-soil interaction into account. The periodic model exploits the periodicity of the track, and applies the Floquet-transform in order to reduce the total infinite model to the finite element model of a reference cell of the tunnel and the boundary element model of the surrounding soil.

In the second subproblem the dynamic soil-structure interaction problem is solved. The structural vibrations due to the incident wave field are computed by means of a three-dimensional coupled finite element-boundary element model, based on the subdomain formulation proposed by Aubry and Clouteau [1, 2]. Here, the structure is modeled using the finite element method, and the dynamic stiffness of the soil is computed using a boundary element soil model based on the Green's functions of a layered half-space.

In the third subproblem, the indoor noise radiated by the structural vibrations is computed using a three-dimensional spectral finite element method applied to rectangular rooms with absorbing boundaries.

The geometry of the problem investigated is plotted in figure 1. A straight underground railway tunnel is placed under a building resting on a layered half space. The origin of the Cartesian coordinate system is located at the center of the building's surface foundation, and the tunnel runs in the y direction.

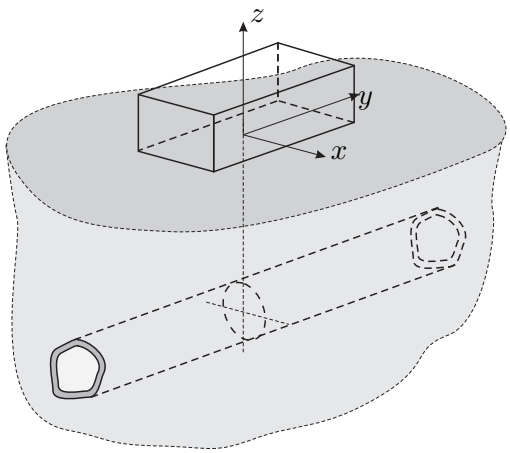

Figure 1: The problem geometry

A weak coupling between the incident wave field and the structural displacements is assumed, meaning that the presence of the building has no effect on the vibration generation mechanism, and the free field displacements are applied as an excitation on the coupled soil-structure model. This assumption is valid, if the distance between the building and the tunnel is large enough in terms of wavelength.

2.1 The incident wave field

The periodicity or invariance of the tunnel and the soil in the longitudinal y direction is exploited using the Floquet transform, limiting the discretization effort to a single bounded reference cell and formulate the problem in the frequency-wavenumber domain [3, 4].

A general analytical formulation is used to compute the response of three-dimensional invariant or periodic media that are excited by moving loads. If the spatial period is L, then the position $\mathbf{x}$ of any point in the problem domain is decomposed as $\mathbf{x} = \tilde{\mathbf{x}} + nL\mathbf{e}_y$, where $\tilde{\mathbf{x}}$ is the position in the reference cell and n is the cell number. The response to moving loads in case of periodic domains is given by [5]:

$$\begin{aligned} \hat{u}_i(\tilde{\mathbf{x}} + n_y L\mathbf{e}_y, \omega) &= \frac{1}{2\pi}\sum_{k=1}^{n}\int_{-\infty}^{\infty} \hat{g}_k(\omega - k_y v)\exp\left[-ik_y(n_y L - y_{k0})\right] \\ &\times \int_{-L/2}^{L/2}\exp\left(-ik_y\tilde{y}'\right)\tilde{\hat{h}}_{zi}(\tilde{\mathbf{x}}', \tilde{\mathbf{x}}, \kappa_y, \omega)\,\mathrm{d}\tilde{y}'\,\mathrm{d}k_y \end{aligned} \tag{1}$$

where $\kappa_y = k_y - 2m\pi/L$ and $k_y = (\omega - \tilde{\omega})/v$. The transfer function $\tilde{\hat{h}}_{zi}(\tilde{\mathbf{x}}', \tilde{\mathbf{x}}, \kappa_y, \omega)$ in the frequency-wavenumber domain is the Floquet transform of the transfer function $\hat{h}_{zi}(\tilde{\mathbf{x}}', \tilde{\mathbf{x}} + n_y L\mathbf{e}_y, \omega)$ in the frequency-spatial domain. This transfer function expresses the response at $\tilde{\mathbf{x}} + n_y L\mathbf{e}_y$ in the $\mathbf{e}_i$ direction due to a unit load applied $\tilde{\mathbf{x}}'$ in the $\mathbf{e}_z$ direction. The summation in the above equation is over the n axles of the train. It can be seen from equation (1) that the transfer function $\tilde{\hat{h}}_{zi}(\tilde{\mathbf{x}}', \tilde{\mathbf{x}}, \kappa_y, \omega)$ and the frequency content of the axle load $\hat{g}_k(\omega)$ are needed to compute the response to moving loads.

The transfer functions are calculated by solving a three-dimensional dynamic tunnel-soil interaction problem, using a finite element (FE) formulation for the tunnel and a boundary element (BE) method for the soil in the reference cell [3, 4].

An invariant tunnel embedded in a layered half space at a depth of 13.5 m is considered. The tunnel has an internal radius $r_i = 2.7$ m and a wall thickness $t = 0.3$ m. The tunnel has a concrete lining with a Young's modulus $E^{\mathrm{t}} = 35000$ MPa, a Poisson's ratio $\nu^{\mathrm{t}} = 0.25$, a density $\rho^{\mathrm{t}} = 2500\,\mathrm{kg/m^3}$ and a hysteretic material damping ratio $\beta^{\mathrm{t}} = 0.02$. A concrete slab is poured on the tunnel invert, which has a Young's modulus $E^{\mathrm{t}} = 28500$ MPa, a Poisson's ratio $\nu^{\mathrm{t}} = 0.2$, a density $\rho^{\mathrm{t}} = 2500\,\mathrm{kg/m^3}$ and a hysteretic material damping ratio $\beta^{\mathrm{t}} = 0.02$. The invariant tunnel is modeled as a periodic structure with a spatial period $L = 0.3$ m. The reference cell is discretized using 8-node volume elements with incompatibility bending modes.

The dynamic soil characteristics are summarized in table 1. The layered half space consists of two layers with a thickness of 2 m and 18.5 m, respectively, on top of a homogeneous half space.

Table 1: Dynamic soil characteristics on line 4, north of Chengfulu station.

Layer	d [m]	C_s [m/s]	C_p [m/s]	E [$\times 10^6$ N/m^2]	ν [$-$]	ρ [kg/m^3]	β [-]
1	2.0	180	360			2000	0.060
2	18.5	220	440			2000	0.050
3	∞	320	640			2000	0.045

The displacement field $\tilde{u}_{\mathrm{t}}(\tilde{\mathbf{x}}, \kappa, \omega)$ in the tunnel is decomposed on a basis of functions $\tilde{\psi}_m(\tilde{x}, \kappa)$, which are periodic of the second kind. Figures 2a and 2b show the two free tunnel modes $\tilde{\psi}_m(\tilde{x}, \kappa)$ at a zero wavenumber. Likewise, the soil displacements $\tilde{u}_{\mathrm{t}}(\tilde{\mathbf{x}}, \kappa, \omega)$ are expressed as the superposition of waves that are radiated by the tunnel into the soil. The weak variational formulation of the problem results in the following system of equations in the frequency-wavenumber domain [2, 3]:

$$\left[\mathbf{K}_{\mathrm{t}}(\kappa) - \omega^2\mathbf{M}_{\mathrm{t}}(\kappa) + \mathbf{K}_{\mathrm{s}}(\kappa, \omega)\right]\boldsymbol{\alpha}(\kappa, \omega) = \mathbf{F}_{\mathrm{t}}(\kappa, \omega) \tag{2}$$

where $\boldsymbol{\alpha}(\kappa,\omega)$ are the unknown modal coordinates. $\mathbf{K}_t(\kappa)$ and $\mathbf{M}_t(\kappa)$ are the dynamic stiffness and mass matrix of the tunnel. $\mathbf{K}_s(\kappa,\omega)$ is the dynamic stiffness matrix of the soil calculated with a periodic boundary element formulation with Green-Floquet functions defined on the periodic structure with period L along the tunnel [2, 6].

A conventional non-ballasted concrete slab track is considered in the tunnel. UIC 60 rails are used that have a cross-sectional area $A_\mathrm{r} = 7.672 \times 10^{-3}\,\mathrm{m}^2$, a moment of inertia $I_\mathrm{r} = 3.039 \times 10^{-5}\,\mathrm{m}^4$, a mass per unit length $\rho_\mathrm{r} A_\mathrm{r} = 60.22$ kg/m and a bending stiffness $E_\mathrm{r} I_\mathrm{r} = 6.382 \times 10^{6}\,\mathrm{Nm}^2$. Soft rail pads with a stiffness $k_\mathrm{rp} = 50\,\mathrm{MN/m}$ discretely support the rails at an interval $d = 0.6$ m on the sleepers. The concrete sleeper has a mass $M_\mathrm{s} = 200$ kg. The track is modeled as an infinite beam on continuous support. The model consists of an infinite Euler beam, representing the (two) rails and the mass elements representing the sleepers. The mass of the sleepers is distributed in the longitudinal direction with a mass per unit length $m_\mathrm{s} = M_\mathrm{s}/d = 333$ kg/m. The rail pads are modeled as a continuous support with vertical stiffness $\bar{k}_\mathrm{rp} = k_\mathrm{rp}/d = 83.3\,\mathrm{MN/m}^2$ between the beam and the sleepers, while the rigid connection between the sleepers and the concrete slab is modeled with very stiff springs below the mass elements.

The Craig-Bampton substructuring technique is used to efficiently incorporate a track in the tunnel, describing the kinematics of the track-tunnel system as a superposition of the track modes on a rigid base and the quasi-static transmission of the free tunnel modes into the track [3, 4]. Figure 2 shows the tunnel modes at zero wavenumber, with their quasi-static transmission into the track and a track mode on a rigid base.

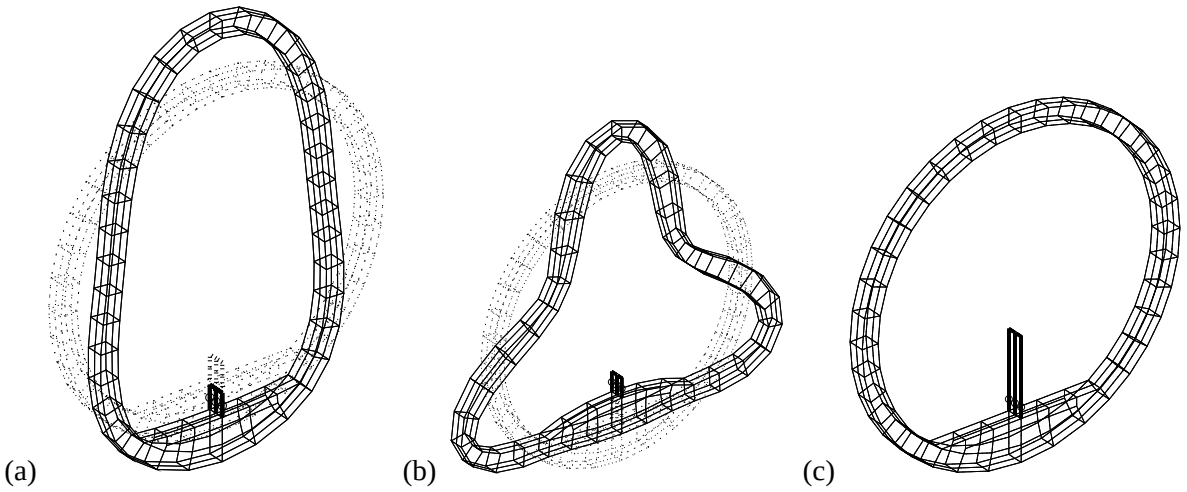

Figure 2: (a,b) The free tunnel modes and quasi-static transmission into the track and (c) a track mode on a rigid base.

Vibrations are generated due to the wheel-rail interaction. In this paper, two excitation mechanisms are considered: the quasi-static excitation and the unevenness excitation. For the quasi-static excitation, the axle loads $g_k(t)$ are constant and equal to the total weight of the train per axle. For the unevenness excitation, the contact force $\hat{\mathbf{g}}(\omega)$ in the frequency domain is calculated by solving the wheel-track interaction problem [7]:

$$[\hat{\mathbf{C}}^\mathrm{v}(\omega) + \hat{\mathbf{C}}^\mathrm{tr}(\omega)]\hat{\mathbf{g}}(\omega) = \hat{\mathbf{u}}_\mathrm{w/r}(\omega) \tag{3}$$

where $\hat{\mathbf{u}}_\mathrm{w/r}(\omega)$ is the combined rail and wheel roughness, $\hat{\mathbf{C}}^\mathrm{v}(\omega)$ is the compliance of the vehicle and $\hat{\mathbf{C}}^\mathrm{tr}(\omega)$ is the compliance of the track in the moving frame of reference. When the train speed is much lower than the critical wave speed in the track-tunnel-soil system, the track compliance $\hat{\mathbf{C}}^\mathrm{tr}(\omega)$ can be computed in the fixed frame of reference.

A metro train traveling with a speed of 50 km/h on an uneven rail is modeled. The train consist of seven cars each of length 16 m. The bogie and axle distance on all cars are 10.34 m and 1.91 m, respectively. The mass of the coach with passengers is 43000 kg, while the mass of the bogie and axle are 3600 kg and 1700 kg,

respectively. The vehicle compliance $\hat{\mathbf{C}}^{\mathrm{v}} = \mathrm{diag}\{-1/(M_u\omega^2)\}$ of order 28, where M_u is the unsprung axle mass.

The rail unevenness $u_{w/r}(y)$ is expressed as a stochastic process characterized by a single-sided power spectral density (PSD) $\tilde{S}_{w/r}(k_y)$ written as a function of wavenumber $k_y = \omega/v = 2\pi/\lambda_y$:

$$\tilde{G}'_{\mathrm{w/r}}(n_y) = \frac{A' n_{y2}^2 (n_y^2 + n_{y1}^2)}{n_y^4 (n_y^2 + n_{y2}^2)} \tag{4}$$

where $n_{y1} = 0.0233$ cycle/m and $n_{y2} = 0.1312$ cycle/m. According to the Federal Railroad Administration (FRA), the track is classified into six classes depending on the rail quality, class 6 track being the best and class 1 the poorest. In this paper, FRA track class 1 is used for which the roughness parameter $A' = 16.72 \times 10^{-7}$ m cycle. An artificial roughness is generated from this PSD curve and the frequency content of roughness is determined for a particular speed [7].

Figure 3 shows the vertical component of the free field incident wave field at the origin of the coordinate system. The dominant part of the frequency content is between 10 and 80 Hz, which gives rise to low-frequency vibrations and re-radiated noise in the buildings. The higher frequency components up to 150 Hz are also present but are considerably attenuated due to the material damping in the soil. The peak in the frequency content around 55 Hz corresponds to the wheel-track resonance frequency. The passage of the individual axles of the train is not apparent in the time history, as the contribution of the quasi-static forces is negligible in the free field and the dynamic forces due to the rail unevenness dominate.

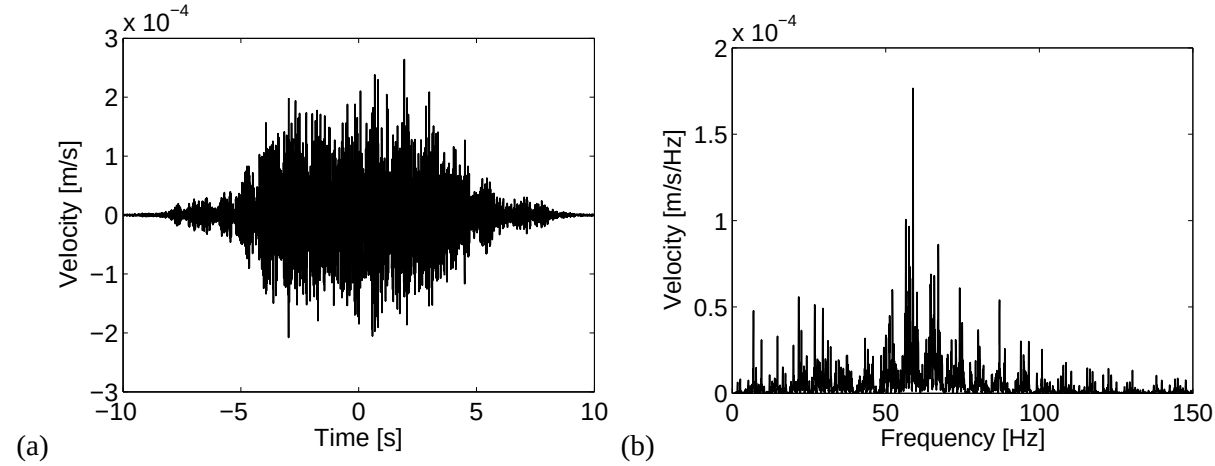

Figure 3: (a) Time history and (b) frequency content of the vertical component of the free field velocity at the center of the surface foundation

2.2 Structural response

The modeled structure is a two-story portal frame office building located directly above the tunnel. The dimensions of the building are 10 m $\times$ 8 m $\times$ 6 m in the x, y and z directions, respectively. The structure is modeled by means of a 3D structural finite element method. The finite element mesh is shown in figure 4(a).

The two story superstructure is supported by a 0.3 m thick reinforced concrete raft foundation. The basic structure consists of a reinforced concrete portal frame structure containing vertical columns of cross sectional dimensions 0.3×0.3 m and horizontal beams of dimensions 0.3×0.2 m. This frame structure supports two 0.3 m thick horizontal slabs. In the first level, the structural model is extended with a reinforced concrete stiffener core. The thickness of the core walls is 0.15 m. The structural model is further extended with the in-fill walls of two rooms (Room 1 and Room 2) in the second storey. Both rooms have dimensions $5 \times 4 \times 3$ m. The masonry in-fill walls are 0.06 m thick. A constant hysteretic structural damping of $\beta_s = 0.025$ is assumed.

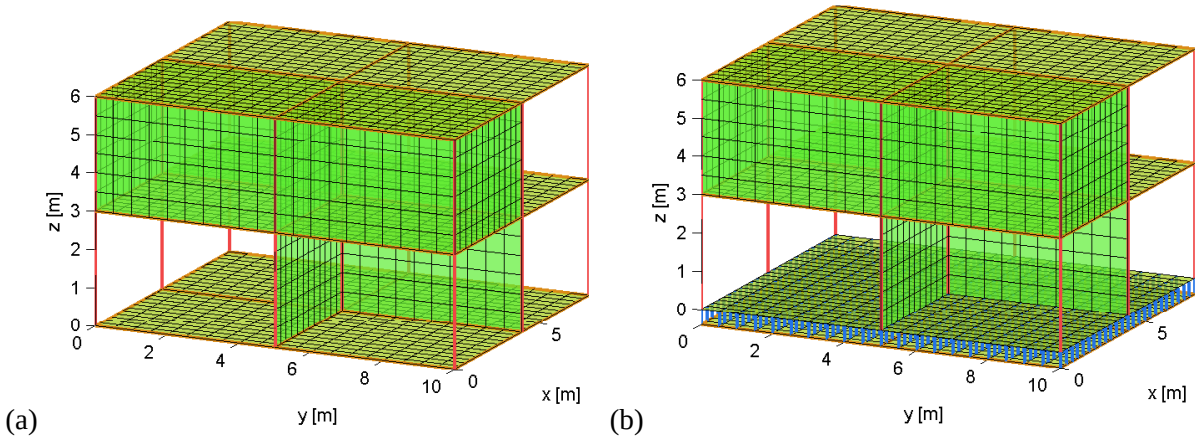

Figure 4: Finite element mesh of the office building (a) without and (b) with base isolation.

The subdomain method proposed by Aubry et al. [1] and Clouteau [8] is used to formulate the dynamic soil-structure interaction problem. The equation of motion of the building is:

$$\left(\begin{bmatrix} \mathbf{K}_{ss} & \mathbf{K}_{sb} \\ \mathbf{K}_{bs} & \mathbf{K}_{bb} + \hat{\mathbf{K}}^{g}_{bb} \end{bmatrix} - \omega^2 \begin{bmatrix} \mathbf{M}_{ss} & \mathbf{M}_{sb} \\ \mathbf{M}_{bs} & \mathbf{M}_{bb} \end{bmatrix} \right) \begin{Bmatrix} \hat{\mathbf{u}}_s \\ \hat{\mathbf{u}}_b \end{Bmatrix} = \begin{Bmatrix} \mathbf{0} \\ \hat{\mathbf{f}}_b \end{Bmatrix} \tag{5}$$

where the structural displacements $\hat{\mathbf{u}}^s$ are separated to the displacement DOF of the foundation $\hat{\mathbf{u}}_b$ and the remaining DOF of the superstructure $\hat{\mathbf{u}}_s$. $\mathbf{M}$ and $\mathbf{K}$ denote the finite element mass and stiffness matrices, and $\hat{\mathbf{K}}^{g}_{bb}$ stands for the frequency dependent dynamic stiffness matrix of the soil, and $\hat{\mathbf{f}}_b$ is the loading force acting on the structure's foundation. This force is due to the incident ground vibrations, and it is computed by means of a 3D boundary element method [8] in the frequency domain, using the Green's functions of a layered half-space [9].

Figures 5-6 display the vertical component of the structural velocity computed in two points of the office building. The first point is located on the foundation at coordinates $x = 2.5$ m, $y = 2$ m, while the second point is located on the floor of Room 1, at the same horizontal coordinates.

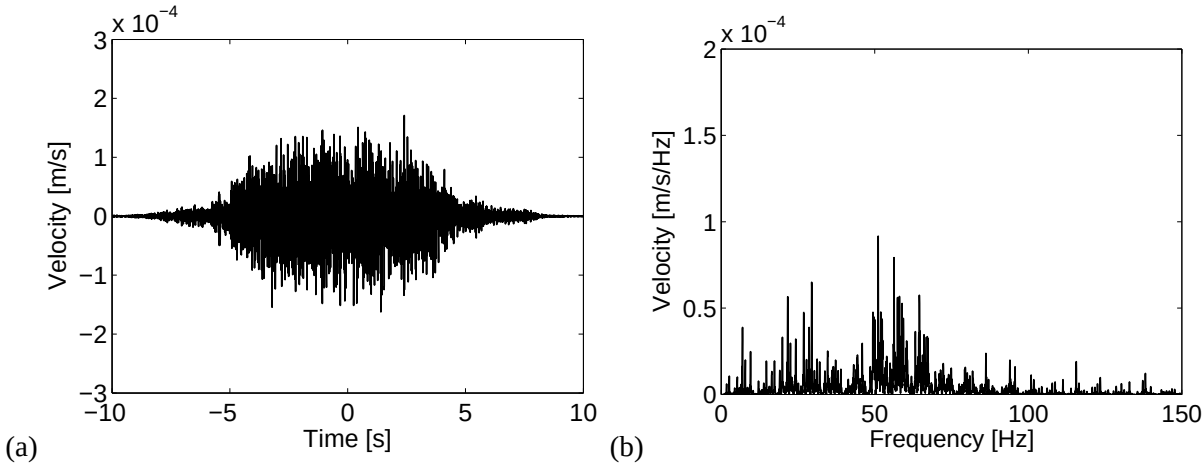

Figure 5: (a) Time history and (b) frequency content of the vertical component of the structural velocity at the foundation of the office building

Comparing the incident wave field at the foundation (figure 3) with the vibration velocity of the foundation (figure 5), the effect of dynamic soil-structure interaction can be investigated. This effect is a slight attenuation of the ground vibrations due to the presence of the office building structure. Figures 5-6 show how

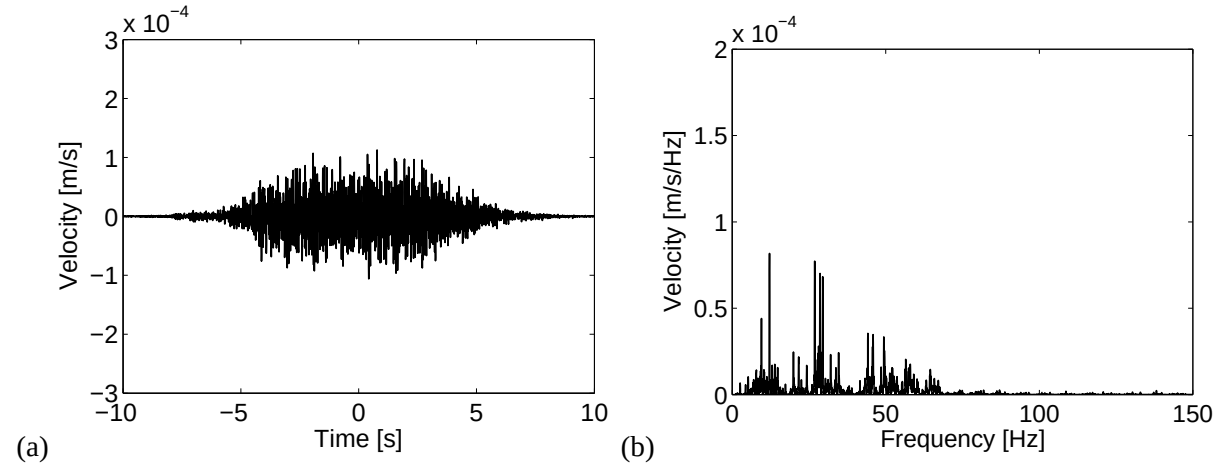

Figure 6: (a) Time history and (b) frequency content of the vertical component of the structural velocity at the first floor of the office building

the structural vibrations change as they propagate from the foundation to the upper levels. In the higher frequency range (above 50 Hz), the structural vibrations are attenuated. This attenuation is due to the structural damping.

2.3 Acoustic response

After determining the structural vibrations, the acoustic response of the closed rooms can be computed. This computation involves the solution of the Helmholtz equation in closed acoustic domains.

As the impedance of the radiating walls is much larger than that of the internal acoustic space, a weak coupling between structural and acoustic vibrations is assumed. The acoustic pressure inside the room has no effect on the vibration of the walls and the computed structural vibration velocity is applied as a boundary condition in an acoustic boundary value problem.

The internal acoustic space of the closed rooms is characterized by the speed of sound $C_a = 343$ m/s and the material density of the air $\rho_a = 1.225$ kg/m^3. The absorbing surfaces of the rooms are characterized by an acoustic impedance relating the acoustic pressure p_a to the difference of normal structural and acoustic velocities $\hat{v}_s$ and $\hat{v}_a$ of the acoustic boundary:

$$\hat{p}_a = Z_a(\hat{v}_s - \hat{v}_a) \tag{6}$$

At relative low frequencies, the acoustic impedance can be computed from the walls' acoustic absorption coefficient α, which gives the ratio of the absorbed and the incident acoustic energy when a normal incident acoustic plane wave is reflected from the surface. In the present paper, an absorption coefficient $\alpha = 0.15$ is assumed. The selected value is typical for absorbing rooms with furniture and carpeted floors.

An acoustic spectral finite element method is used, in which the internal pressure $\hat{p}_a(\mathbf{x}, \omega)$ is expressed in terms of acoustic room modes:

$$\hat{p}_a(\mathbf{x}, \omega) = \sum_n \Psi_n(\mathbf{x}) \hat{\beta}_n(\omega) \tag{7}$$

where $\Psi_n(\mathbf{x})$ denotes the n-th acoustic mode of the shoe-box shaped interior domain with rigid boundary conditions and $\hat{\beta}_n(\omega)$ is the corresponding modal coordinate.

The application of the spectral finite element method results in a system of linear equations for the acoustic modal coordinates $\hat{\beta}_n$:

$$\left(\mathbf{\Lambda} + \mathrm{i}\omega\mathbf{D} - \omega^2\mathbf{I}\right)\hat{\boldsymbol{\beta}} = \mathrm{i}\omega\hat{\mathbf{F}} \tag{8}$$

where $\mathbf{\Lambda} = \text{diag}\left\{\omega_n^2\right\}$ contains the eigenfrequencies of the acoustic domain, $\mathbf{I}$ is a unit matrix, $\mathbf{D}$ denotes the modal damping matrix related to the wall absorption, and $\hat{\mathbf{F}}$ denotes the modal load vector. The elements of the matrix $\mathbf{D}$ are defined by

$$D_{nm} = \rho_a C_a^2 \int_{\Gamma_a} \frac{\Psi_n \Psi_m}{Z_a} \mathrm{d}\Gamma \tag{9}$$

where n and m are the column and row indices, respectively, and the n-th element of the vector $\mathbf{F}$ is given by

$$\hat{F}_n = \rho_a C_a^2 \int_{\Gamma_a} \Psi_n \hat{v}_s \mathrm{d}\Gamma \tag{10}$$

For the case of constant wall absorption on the boundary, the values D_{nm} can be expressed analytically. Moreover, the off-diagonal elements can be truncated with a relative small error [10], resulting in a very fast algorithm for the acoustic computations. In this case the spectral finite element method results in a direct boundary integral representation of the acoustic modal coordinates.

In the present paper, the total acoustic sound energy E inside the closed rooms is used to characterize the acoustic response. This characterization has the advantage that it gives a global estimate of the acoustic response for the whole acoustic domain, so the error resulting from evaluating the sound pressure at single points where local attenuation or amplification occurs, can be avoided.

The sound energy is defined as

$$\hat{E} = \frac{1}{4\rho_a C_a^2} \int_{\Omega_a} \left(|\hat{p}(\mathbf{x})|^2 + \left(\frac{C_a}{\omega}\right)^2 \nabla \hat{p}(\mathbf{x}) \cdot \nabla \hat{p}(\mathbf{x}) \right) \mathrm{d}\Omega_a \tag{11}$$

and is efficiently computed from the acoustic modal coordinates as

$$\hat{E} = \frac{1}{4\rho_a C_a^2} \sum_n |\hat{\beta}_n|^2 \left[1 + \left(\frac{\omega_n}{\omega}\right)^2 \right] \tag{12}$$

The one-third octave band spectra of the acoustic sound energy due to the passage of the metro train is displayed in figure 7. The dominant one-third octave bands are determined by the acoustic room modes. In the rectangular domain these modes can be given by the number of half wavelengths in the three coordinate directions. For the case of room 1, the first acoustic mode (1, 0, 0) appears at 28.58 Hz, the second mode (0, 1, 0) appears at 34.3 Hz. The first vertical mode (0, 0, 1) can be found at 61.25 Hz. The correspondence between these eigenfrequencies and the dominant one-third octave bands is clearly visible in the figure even for the relative large wall absorption. The sharp peak in the 63 Hz one-third octave band is due to the coincidence of the wheel-track resonance frequency and the first vertical acoustic room mode.

3 Vibration and noise isolation

In the following, the numerical model will be used to quantify the effect of different vibration and noise mitigation countermeasures. Three measures will be considered: the application of a floating slab track, the application of base isolation and finally, a box-within-box arrangement.

A useful way to evaluate the effectiveness of the isolation measure is to take the ratio of the response with and without isolation. A common measure of this ratio is the insertion gain in dB, which indicates the increase in vibration levels caused by the modifications. This measure is negative for the case of vibration reduction and positive for vibration increase. The insertion gain is defined as the ratio of the response u^{iso} of the isolated and the response u^{uniso} unisolated system as:

$$\text{IG[dB]} = 20 \log_{10} \left(\frac{u^{\text{iso}}}{u^{\text{uniso}}} \right) \tag{13}$$

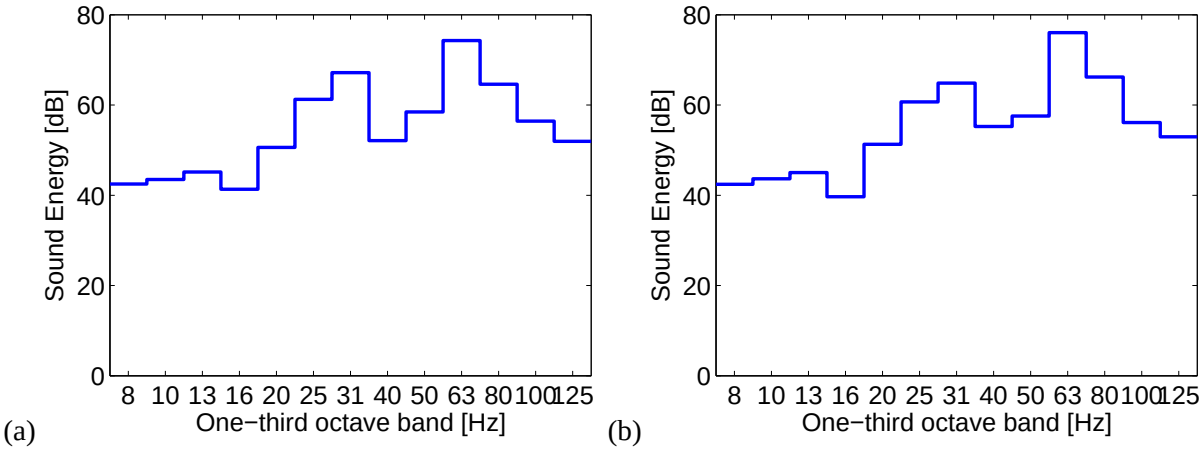

Figure 7: One-third octave band levels of the sound energy in (a) Room 1 and (b) Room 2 due to the passage of the metro train.

3.1 Countermeasure 1

Firstly, the isolation of the source is considered to mitigate the vibrations induced by moving trains. This has an advantage with respect to the isolation on the receiver side that it benefits multiple structures in the surrounding.

In this paper, the vibration isolation efficiency of a floating slab track with an isolation frequency of 10 Hz is investigated. The concept of isolation frequency is widely used and it defines the isolation frequency as the resonance frequency of a single-degree-of-freedom system with a mass equal to the track's mass per unit length and stiffness equal to the vertical stiffness of the slab bearings. Discontinuous concrete slabs of dimensions $31\ \text{m} \times 2.7\ \text{m} \times 0.5\ \text{m}$ are supported by two rows of 17 springs with a spring stiffness of 12 MN/m each. The slab is modeled as a continuous beam coupled to the tunnel via a uniform support, that has a low stiffness corresponding to the isolation frequency of 10 Hz.

The coupled periodic FE-BE model is again used to compute the incident wave field. It should be mentioned that the track is incorporated in the tunnel using the Craig-Bampton substructuring and therefore, it is not required to recompute the soil's dynamic stiffness as it only depends on the tunnel modes. This procedure adds to the versatility of the approach and facilitates the future parametric studies on different isolation measures in the tunnel.

Figure 8 shows the insertion gain in the frequency domain at the origin when a 10 Hz floating slab track is considered. The insertion gain is based on the comparison of the transfer functions in the case of the isolated and unisolated track. The insertion gain becomes negative at frequencies greater than 15 Hz, indicating the isolation.

For a more relevant assessment, the response to moving loads is computed after installing a floating slab track. Figure 9 shows the time history and the frequency content of the vertical vibration velocity at the origin for the passage of the train on the isolated track. It can be observed that the vibration levels have significantly reduced above 15 Hz. This can be explained by the fact that above the isolation frequency energy remains confined to the slab and propagates along the slab instead of being transmitted to the tunnel and the soil. At frequencies below 15 Hz, however, no benefit is achieved, instead vibration levels have increased. Although these low frequency vibrations can cause malfunctioning of sensitive equipment in nearby buildings, they are not important from the perspective of re-radiated noise.

Figure 10 compares the vibrations due to a passage of a train in the isolated and unisolated case in one-third octave bands. The maximum vibration levels in case of the unisolated track are observed around the wheel-track resonance frequencies, which are completely attenuated by installing a floating slab track. Around the wheel-track resonance 35 dB reduction in the vibration levels is achieved.

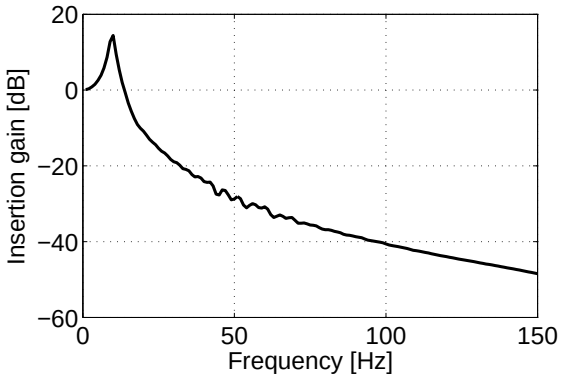

Figure 8: Insertion gain at the origin for the case of a floating slab track with an isolation frequency of 10 Hz.

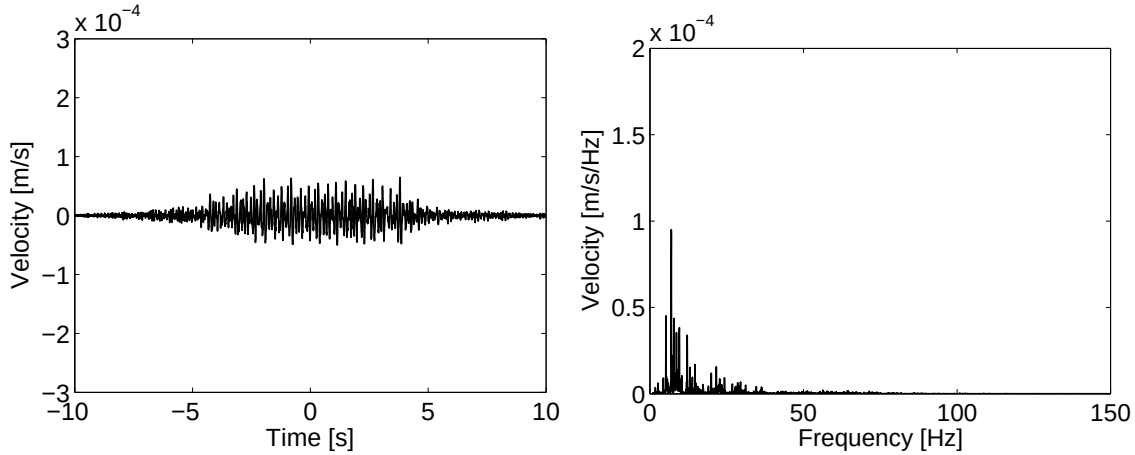

Figure 9: (a) Time history and (b) frequency content of the vertical vibration velocity at the origin for the passage of the metro train running on a floating track

Finally, re-radiated noise is predicted in Room 1 due to the passage of the train in the tunnel for the isolated case. In the case of the unisolated track, the maximum sound energy level is observed in 63 Hz band, which is perceived by humans as a rumbling noise inside the rooms. About 35 dB reduction is achieved by installing a floating slab track, which clearly demonstrates its efficiency. The human ear perceives sound above 20 Hz, but as the ear's sensitivity is much smaller in the range between 20 Hz and 50 Hz than above 50 Hz, the total noise reduction achieved by the floating slab track is larger than 30 dB.

3.2 Countermeasure 2

The second investigated countermeasure is base isolation of the office building, where the superstructure is dynamically isolated from the foundation. In the present case, this dynamical isolation is performed by inserting a new slab between the columns of the first level and the original foundation slab, and placing an elastic material between the new and the foundation slab, as can be seen in Figure 4(b). The isolation frequency of the base isolation is defined as the resonance frequency of the SDOF system consisting of the total mass m of the superstructure with the new slab and the total stiffness k of the springs.

In the present example, the elastic material is modelled by distributed springs acting between the foundation and the slab nodes. The stiffness of the springs is defined so that the total stiffness results in a required resonance frequency $f_z = 5$ Hz, and the vertical static displacement of the new slab is uniform with respect

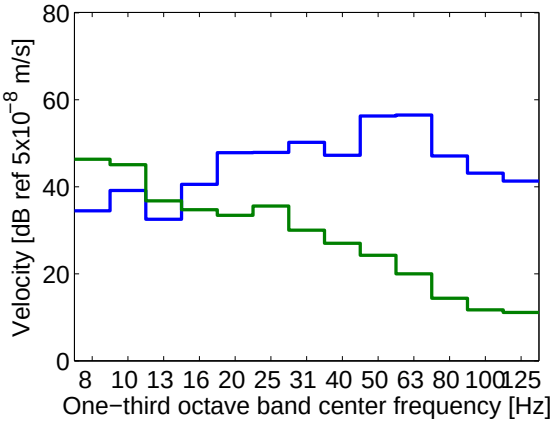

Figure 10: Vertical vibration velocity levels at the foundation of the building for the unisolated case (blue) and for the isolation with the floating slab track (green).

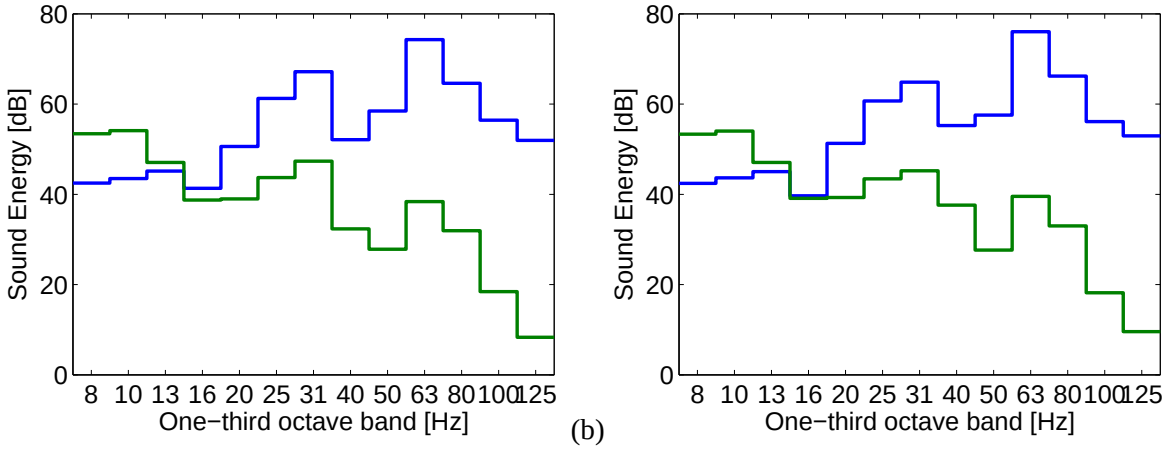

Figure 11: One-third octave band spectrum of the sound energy in (a) Room 1 and (b) Room 2 due to the passage of the metro running on the floating slab track. Unisolated case marked with blue, isolated case with green.

to the horizontal coordinates.

Figure 12 displays the vertical structural velocity in the base isolated building at the floor of Room 1. Comparing this vibration level with the velocity in the unisolated case (figure 6), the effect of base isolation is clearly observable. Figure 13(a) displays the velocity levels in one-third octave bands. The reduction is about 10-15 dB around the wheel-track resonance frequency, and increases to 20 dB in the higher frequency range. The same holds for the noise isolation, as can be seen in figure 13(b).

3.3 Countermeasure 3

A third noise isolation method is also investigated. The method, widely used in acoustic laboratories, smaller concert halls or theater rooms for both vibration and noise reduction purposes, is a box-within-box arrangement, where the whole interior boundary of a room is dynamically isolated from the vibrations of the building's walls and slabs. This rather expensive method results in local vibration and noise isolation of the building's room.

In the model presented in tis paper, the internal box consists of a 10 cm wide concrete floor slab and 6 cm wide concrete walls surrounded by a resilient material. For the sake of simplicity, this material has been modeled by a continuous spring-damper system, where the springs are connected to each node of the plate

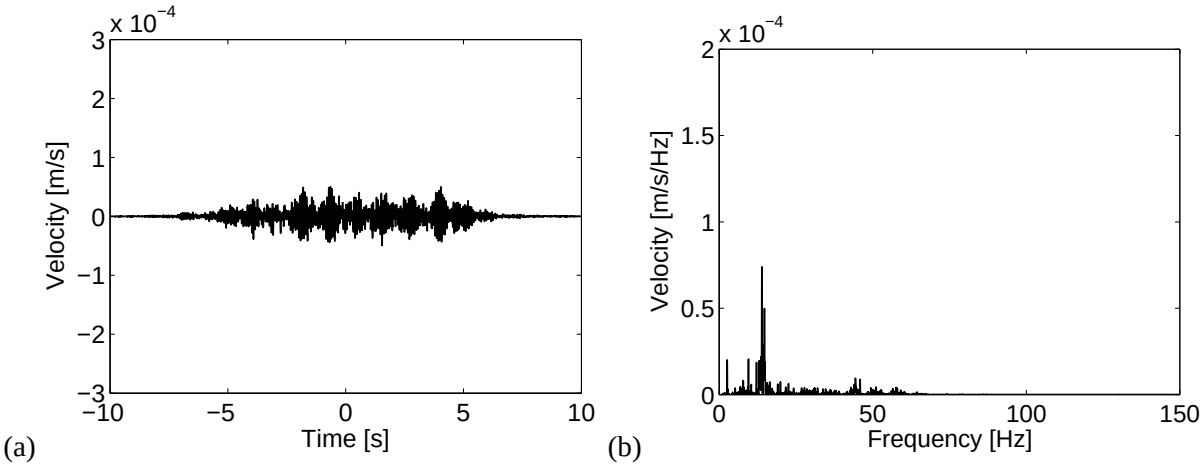

Figure 12: (a) Time history and (b) frequency content of the vertical structural velocity in the base isolated building at the floor of Room 1 due to the passage of the metro train.

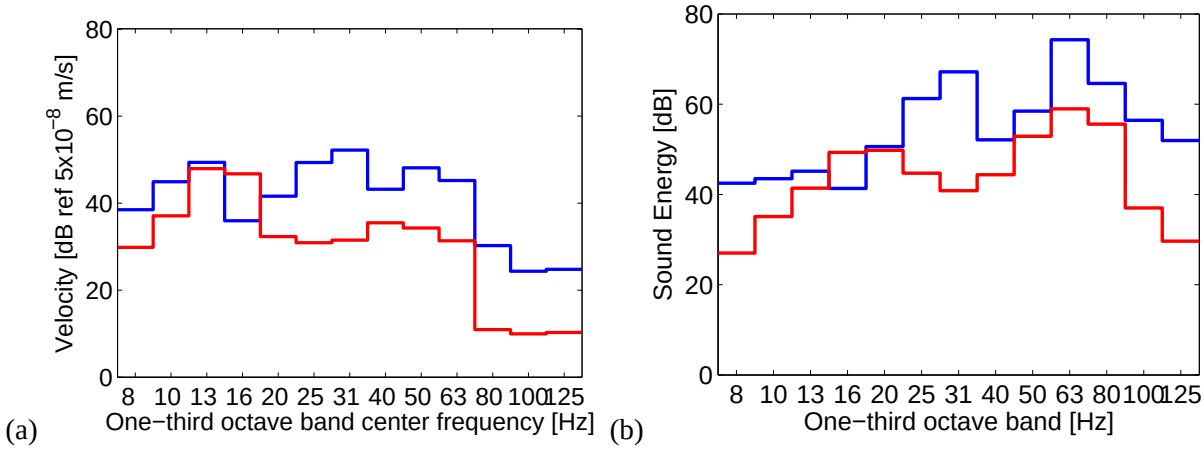

Figure 13: One-third octave band levels of the (a) vertical vibration velocity at the floor of Room 1 and of the (b) sound energy in Room 1 in the unisolated (blue) and in the base isolated building (red).

elements representing the floor and the walls. Similarly, the ceiling is modeled as a 6 cm thick wooden slab covered with a resilient material. The vertical isolation frequency of the room on springs have been chosen to 10 Hz and the horizontal resonance has been chosen to 8 Hz.

Figure 14 displays the acoustic response in Room 1 and Room 2 to the passage of the metro train, for the case of the acoustic isolation with the box-within-box arrangement. The noise reduction is rather weak in the lower frequency range, but at the critical wheel-track resonance frequency, in the 63 Hz band, 25 dB reduction is achieved. In the higher frequency range, the reduction exceeds 30 dB.

3.4 Comparison of the three isolation methods

In the following, the noise isolation efficiency of the three reduction methods is compared. Figure 15 displays the insertion gain computed from the re-radiated noise in Room 1 for all the three noise isolation countermeasures.

Considering that the noise reduction is more important above 40 Hz, the floating slab track is the most effective countermeasure, providing vibration isolation of the total building and the surrounding structures. However, one must not forget that the application of this method may result in large vibration and noise increase in the track and the metro train. The investigation of these effects is beyond the scope of the present

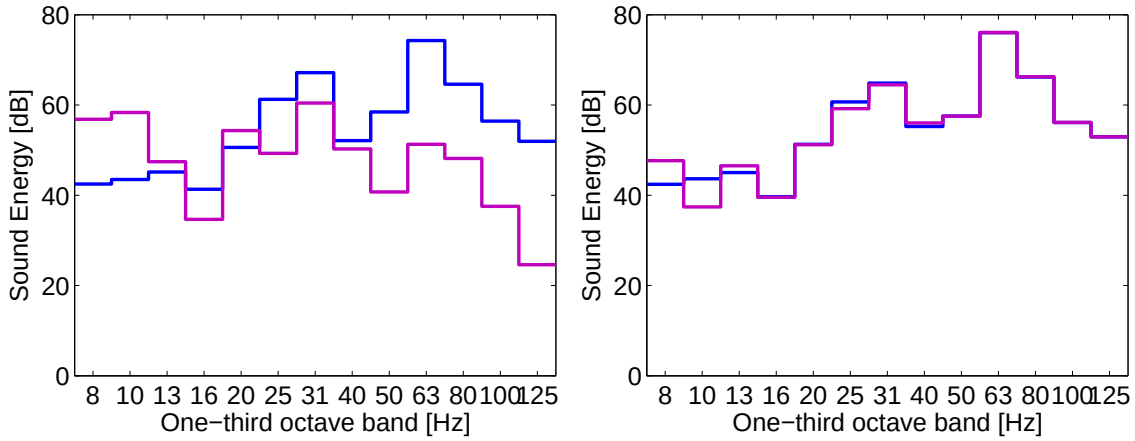

Figure 14: One-third octave band levels of the sound pressure in (a) Room 1 with the box-within-box arrangement and (b) in Room 2 due to the passage of the metro train. The unisolated case is shown with blue, the isolated case with magenta

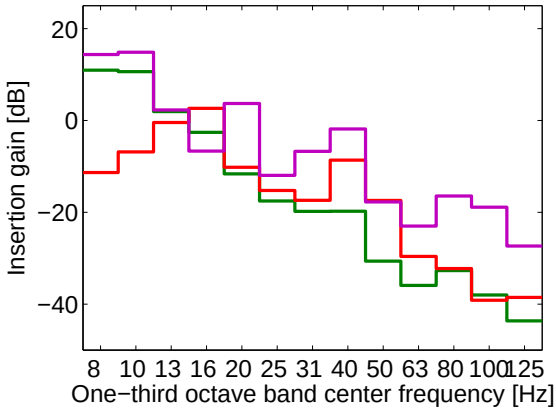

Figure 15: Insertion gain computed from the re-radiated noise in Room 1 due to the passage of the metro train for the floating slab track (green), the base isolation (red) and the box-within-box arrangement (magenta).

paper. The base isolation of the structure is the second most effective noise isolation, exceeding 30 dB above 100 Hz. However, this amount of vibration reduction is still less than predicted by a single degree of freedom (SDOF) system. This difference is due to the fact that the complex superstructure does not behave as a rigid body on springs at higher frequencies. Due to the flexibility and internal vibrations of the building, the total mass of the superstructure is not experienced by the isolation springs, what reduces the effectiveness of the base isolation. In the present case, the poorest countermeasure is the base isolation of the building, still providing 20 dB reduction at high frequencies. For the case of the simple internal box structure, the effect of the flexibility of the box structure is less pronounced than for the case of the base isolation.

4 Conclusions

A numerical model has been presented that is used to compute structural vibrations and re-radiated noise in buildings generated by underground railway traffic. The model is a deterministic three-dimensional approach, accounting for vibration generation by a moving train on periodic media, dynamic soil-structure interaction and sound radiation into closed rooms.

The methodology has been used to demonstrate the efficiency of three vibration and noise reduction methods: a floating slab track, base isolation and noise isolation with a box-within-box arrangement. The countermea-

sures have been compared by terms of insertion gain computed from the re-radiated noise.

The floating slab track has been found as the most effective vibration and noise reduction mechanism. This method provides the largest amount of vibration reduction in the investigated building, and it yields a vibration reduction at the source what is advantageous to all the structures around the metro line. It has been found that base isolation of the structure can result in significant vibration isolation over all the building, but, for the case of complex structures, the isolation effect is less than predicted by SDOF systems. This conclusion is significant, as mass-spring systems form the basis of the planning of base isolation systems in lots of the practical cases. The appication of the box-within-box arrangement resulted in less noise reduction than the base isolation. This method is relative expensive, as it reduces the vibrations of a single room only.

References

[1] D. Aubry and D. Clouteau. A subdomain approach to dynamic soil-structure interaction. In V. Davidovici and R.W. Clough, editors, *Recent advances in Earthquake Engineering and Structural Dynamics*, pages 251–272. Ouest Editions/AFPS, Nantes, 1992.

[2] D. Clouteau, D. Aubry, M.L. Elhabre, and E. Savin. Periodic and stochastic BEM for large structures embedded in an elastic half-space. In *Mathematical Aspects of Boundary Element Methods*, pages 91–102. CRC Press, London, 1999.

[3] D. Clouteau, M. Arnst, T.M. Al-Hussaini, and G. Degrande. Free field vibrations due to dynamic loading on a tunnel embedded in a stratified medium. *Journal of Sound and Vibration*, 283(1–2):173–199, 2005.

[4] G. Degrande, D. Clouteau, R. Othman, M. Arnst, H. Chebli, R. Klein, P. Chatterjee, and B. Janssens. A numerical model for ground-borne vibrations from underground railway traffic based on a periodic finite element - boundary element formulation. *Journal of Sound and Vibration*, 293(3-5):645–666, 2006. Proceedings of the 8th International Workshop on Railway Noise, Buxton, U.K., 8-11 September 2004.

[5] S. Gupta, G. Degrande, H. Chebli, D. Clouteau, M.F.M. Hussein, and H. Hunt. A coupled periodic fe-be model for ground-borne vibrations from underground railways. In Mota Soares C.A., editor, *Proceedings of the 3th European Conference on Computational Mechanics*, Lisbon, Portugal, June 2006.

[6] D. Clouteau, M.L. Elhabre, and D. Aubry. Periodic BEM and FEM-BEM coupling: application to seismic behaviour of very long structures. *Computational Mechanics*, 25:567–577, 2000.

[7] G. Lombaert, G. Degrande, J. Kogut, and S. François. The experimental validation of a numerical model for the prediction of railway induced vibrations. *Journal of Sound and Vibration*, 2006. Accepted for publication.

[8] D. Clouteau. *MISS Revision 6.2, Manuel Scientifique*. Laboratoire de Mécanique des Sols, Structures et Matériaux, Ecole Centrale de Paris, 1999.

[9] J.P. Wolf. *Dynamic soil-structure interaction*. Prentice-Hall, Englewood Cliffs, New Jersey, 1985.

[10] H.R. Pota. Acoustical room transfer functions without using green's functions. In *Proceedings of the 40th IEEE Conference on Decision and Control*, Orlando, Florida, December 2001.